Int. J. Solids Structures Vol. 29, No. 13, pp. 1657–1675, 1992
Printed in Great Britain.

0020–7683/92 $5.00+ .00

CRACKING OF THIN BONDED FILMS IN RESIDUAL TENSION

J. L. BEUTH, JR
Division of Applied Sciences, Harvard University, Cambridge, MA 02138, U.S.A.

(*Received* 2 *March* 1991; *in revised form* 5 *November* 1991)

Abstract—Solutions are obtained for two elastic plane strain problems relevant to the cracking of a thin film bonded to a dissimilar semi-infinite substrate material. The first problem is that of a crack in the film oriented perpendicular to the film/substrate interface with the crack tip touching the interface. The second problem is that of a crack of the same geometry, but with length less than the film thickness, so that the crack tip is within the film. These problems are used to model several modes of crack extension in thin films bonded to thick substrate materials. Complete results from the solution of each problem are given over the full range of practical elastic mismatches. Dimensionless quantities important in describing the cracking of thin films are introduced and accurate approximate formulas based on the solution results are given for them. Applications are discussed, including criteria for avoiding thin film crack extension and a formula for the curvature change induced by the cracking of a thin film bonded to a substrate of finite thickness. The solution results, approximate formulas and information on their application provide the details necessary for the analysis of practical thin film cracking problems.

1. INTRODUCTION

The two problems solved here are shown in Fig. 1. Both of the elastic plane strain problems studied concern a single crack in an isotropic film (material 1) of thickness h, which is bonded to a semi-infinite isotropic substrate (material 2). In the fully cracked film problem (Fig. 1a), the crack is oriented perpendicular to the film/substrate interface and has length h so that its tip touches the interface. The partially cracked film problem illustrated in Fig. 1b models a crack of identical geometry, but with length a, so that the crack tip is within the film (i.e. $a < h$). In both the fully cracked and partially cracked film problems, the crack faces are subject to uniform pressure loading, σ, which from a fracture mechanics standpoint is equivalent to a traction-free crack in a film supporting a uniform tensile stress σ prior to introduction of the crack. The tensile stress σ can be a residual stress in the film, such as a residual thermal stress, or an applied stress. Fracture mechanics quantities obtained from the solution of these two problems are used here to predict the cracking behavior of thin films bonded to thick substrate materials.

The work of Gecit (1979), Lu and Erdogan (1983a,b), Civilek (1985) and Suo and Hutchinson (1989, 1990), which represents only a portion of that done in the field, has served as the basis for obtaining the two problem solutions outlined in this study. Gecit (1979) outlines solution procedures for problems that include the two analysed in the current study, and presents solution results for some representative material combinations.

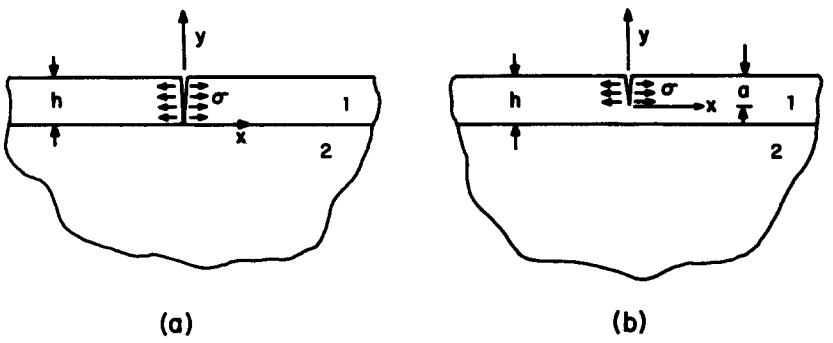

Fig. 1. (a) Fully cracked film; (b) Partially cracked film problems.

Lu and Erdogan (1983a,b) go further by presenting the theory and results for the solution of numerous problems of cracks in a bimaterial strip. As in the work of Gecit (1979), their emphasis is placed on outlining the solution method and presenting results for select material combinations. In more recent work, Civilek (1985) provides the general solution procedure to the problem of one or more cracks in a finite strip of a single material. The solution and analysis of the problems of cracks lying on the interface and in the substrate of a bimaterial strip are detailed by Suo and Hutchinson (1989, 1990). The dislocation formulation and solution procedure applied to solve the bimaterial problems in this study closely follow those used by Civilek (1985) and Suo and Hutchinson (1989, 1990). To avoid a repetition of these earlier formulations, only a brief outline of the solution methods used here is provided in the Appendix.

Because there exists work in the literature offering special solutions to problems similar to those in this study, the main emphasis here is placed on application of the solution procedures to fully map out the dependence of the critical fracture mechanics quantities controlling thin film cracking behavior on the properties of the film/substrate system. For the most part, numerical results existing in the literature are limited to a few special cases (e.g. specific elastic mismatches). Results which are sufficiently complete and general to be useful in applications are not available. To address the current need for such results, this paper presents solutions to the problems illustrated in Fig. 1 over the entire range of practical elastic mismatches. Fracture mechanics quantities extracted from the solutions are used to model not only 2-D in-plane cracking but also 3-D channelling of a crack across the film surface (look ahead to Fig. 3). Results for the fully cracked film problem are plotted and tabulated as a function of the material mismatch parameters. A simple approximate formula is introduced for the partially cracked film problem to make its results more usable. In Section 4, details are given concerning how the results from Sections 2 and 3 can be applied, first, to predict general film cracking behavior and, second, to specifically address the influence of cracking on the use of curvature methods for determining the residual stress in thin bonded films.

A substantial simplification in expressing the material dependence of both problems outlined in this study comes from the work of Dundurs (1969). His work shows that for any problem of a composite body made of two isotropic, elastic materials with prescribed tractions, the material dependence of the problem is reduced from three dimensionless parameters to the two "Dundurs parameters" α and β. For plane strain problems α and β are given by

$$\alpha = \frac{\bar{E}_1 - \bar{E}_2}{\bar{E}_1 + \bar{E}_2}, \quad \beta = \frac{\mu_1(1-2\nu_2) - \mu_2(1-2\nu_1)}{2\mu_1(1-\nu_2) + 2\mu_2(1-\nu_1)}, \tag{1}$$

where $\bar{E} = E/(1-\nu^2)$ is the material plane strain tensile modulus and μ is the material shear modulus. For material 1 having the same properties as material 2, $\alpha = \beta = 0$. For dissimilar materials, switching the 1-2 designation of the materials changes the sign of both α and β. It is clear from (1) that α can vary from -1 to $+1$. In addition, the physically admissible range of β with respect to α can be obtained by restricting μ to be positive and requiring $0 \leqslant \nu \leqslant \frac{1}{2}$ (Dundurs, 1969). This results in the restriction that $|\alpha - 4\beta| \leqslant 1$. Furthermore, the compilation by Suga *et al.* (1988) indicates that for most practical material combinations, values of β typically lie between $\beta = 0$ and $\beta = \alpha/4$. Although the β parameter *can* have significant influence, for most problems studied the role of α is more important than that of β. Because of this, the material dependence of the results presented in this paper is given in terms of α, with $\beta = 0$ and $\beta = \alpha/4$. For problems where a significant β dependence is evident, interpolation to the correct value of β between the practical limits of $\beta = 0$ and $\beta = \alpha/4$ is possible.

2. FULLY CRACKED FILM PROBLEM

Problem description and analysis

For the fully cracked film problem, with its crack tip at the interface (Fig. 1a), the tractions just ahead of the crack tip are of the form

Table 1. Crack tip singularity exponent, s, as a function of α for $\beta = 0$ and $\beta = \alpha/4$

α	−0.99	−0.80	−0.60	−0.40	−0.20	0.0
$\beta = 0$	0.4059	0.4173	0.4318	0.4496	0.4718	0.5000
$\beta = \alpha/4$	0.3121	0.3504	0.3882	0.4249	0.4616	0.5000
α	0.20	0.40	0.60	0.80	0.99	
$\beta = 0$	0.5364	0.5843	0.6495	0.7450	0.9417	
$\beta = \alpha/4$	0.5421	0.5912	0.6535	0.7438	0.9399	

$$\sigma_{xx}(0, y) = C_1 \frac{\sigma h^s}{(-y)^s}, \tag{2}$$

where C_1 is nondimensional and a function of α and β only. The stress singularity exponent, s, is a function of α and β and satisfies the following equation derived by Zak and Williams (1963):

$$\cos(s\pi) - 2\frac{\alpha-\beta}{1-\beta}(1-s)^2 + \frac{\alpha-\beta^2}{1-\beta^2} = 0, \tag{3}$$

where a value of $s = 1/2$ results for the case of identical film and substrate materials. Values of s as a function of α for $\beta = 0$ and $\beta = \alpha/4$ are given in Table 1 and plotted in Fig. 2. For the geometry illustrated in Fig. 1a, the mode I stress intensity factor is defined in this study as

$$K_I \equiv \lim_{y \to 0^-} [(-2\pi y)^s \sigma_{xx}(0, y)], \tag{4}$$

where K_I clearly has dimensions stress · (length)^s. In the case of no elastic mismatch, this generalized stress intensity factor simplifies to the conventional fracture mechanics definition for K_I with units stress · (length)$^{1/2}$.

The fully cracked film solution obtained in this study is used to analyse thin film cracking problems by introducing the following dimensionless quantities:

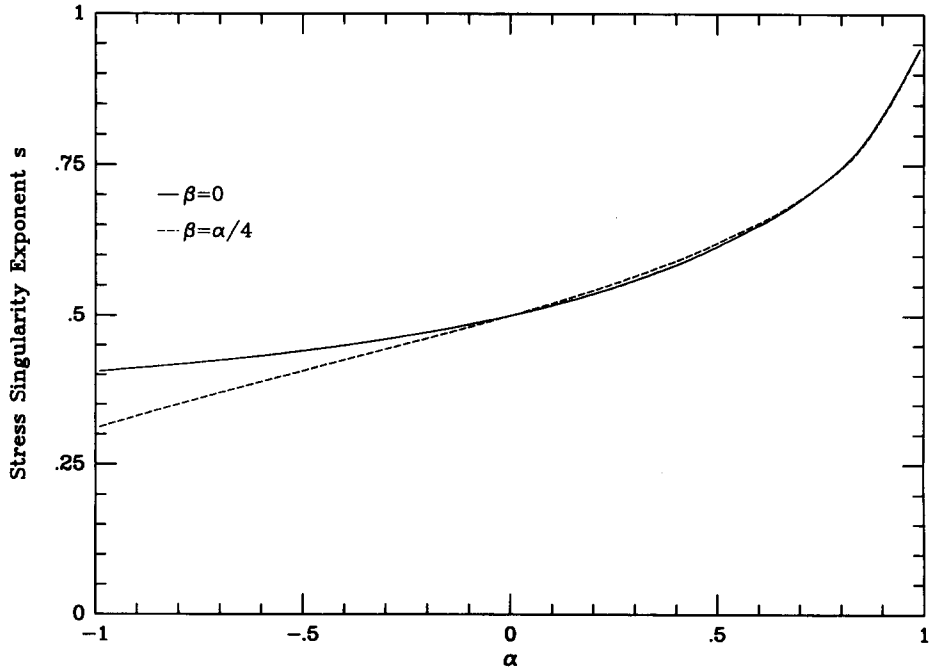

Fig. 2. Plot of crack tip singularity exponent, s, vs α for $\beta = 0$ and $\beta = \alpha/4$.

$$f(\alpha,\beta)=\frac{K_I}{\sigma(\pi h)^s},\quad g(\alpha,\beta)=\frac{\int_0^h \delta(y)\,dy}{\pi\frac{\sigma}{\bar{E}_1}h^2},\quad \delta^*(\alpha,\beta)=\frac{\delta(h)}{\frac{\sigma}{\bar{E}_1}h}. \tag{5}$$

The first quantity, $f(\alpha,\beta)$, is a nondimensionalized stress intensity factor. For a film/substrate combination having no elastic mismatch, $f(0,0) = 1.1215$, the value for an edge crack in a homogeneous half-plane (Tada *et al.*, 1985). The third quantity, $\delta^*(\alpha,\beta)$, is a nondimensionalized crack opening displacement evaluated at the top edge of the crack ($y = h$). For no elastic mismatch, $\delta^*(0,0) = 5.816$ (Tada *et al.*, 1985). The opening displacement of the crack faces at $y = h$ is a commonly measured experimental quantity. Values of δ^* are extracted from the analysis and presented here to allow correlation of the analysis with experiments.

The second quantity given in (5) is a nondimensionalized integral of the crack opening displacement. For the case of no elastic mismatch, $g(0,0) = (1.1215)^2$. This result can be obtained by noting that ΔE, the change in elastic energy per unit depth in the film/substrate system due to the introduction of the crack, must be given by

$$\Delta E=\frac{\sigma}{2}\int_0^h \delta(y)\,dy. \tag{6}$$

Moreover, ΔE must satisfy the relation

$$\Delta E=\int_0^h \mathcal{G}\,da, \tag{7}$$

where $\mathcal{G}$ is the mode I energy release rate, which equals $K_I^2/\bar{E}$ for the case of no elastic mismatch. Substituting $K_I = 1.1215\sigma\sqrt{\pi a}$ into (7), equating with (6), and using the definition of $g(\alpha,\beta)$ in (5) gives $g(0,0) = (1.1215)^2$.

The dimensionless quantity g is introduced because of its relation to two physically significant quantities. In the section on applications, it is shown that $g(\alpha,\beta)$ can be related to the change in curvature of a film/substrate wafer due to the introduction of a film crack. The quantity to be discussed here is the steady-state energy release rate, $\mathcal{G}_{ss}$, of the 3-D crack as it channels across the film (Fig. 3). This mode of crack extension is described in detail by Hutchinson and Suo (1990). As the crack channels across the film, the crack front assumes a curved shape so that the energy release rate, $\mathcal{G}$, is the same at all points along it.

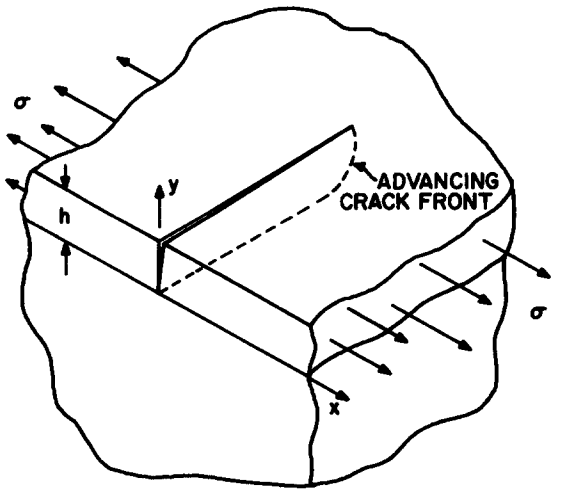

Fig. 3. Steady-state crack channelling across the film for the fully cracked film problem.

For short channel lengths, the crack front shape and $\mathscr{G}$ change as the crack extends. However, for sufficiently long channelling cracks, a steady state is achieved so that the crack front shape and $\mathscr{G}$ remain constant. For such channelling cracks the steady-state energy release rate along the crack front, $\mathscr{G}_{ss}$, can be obtained without having to resort to a 3-D analysis and without having to account for crack front shape. Very recent work by Nakamura and Kamath (1991) indicates that steady-state conditions are quickly achieved by channelling cracks. They present a full 3-D analysis of crack channelling for the special case of a film bonded to a rigid substrate (i.e. $\alpha = -1$). Their results show that in this limiting case, steady-state conditions are achieved by channelling cracks having lengths about twice the film thickness.

For the steady-state condition, the total work release per unit length of crack propagation can be arrived at by subtracting the energy stored in a unit slice far behind the crack front from that of a unit slice far ahead of the crack front. This total work release per unit crack propagation is simply the quantity ΔE given in (6). The quantity $\Delta E/h$ must therefore equal the energy release rate of the channelling crack, $\mathscr{G}_{ss}$. Using the definition of $g(\alpha, \beta)$ in (5), yields the following formula for the mode I steady-state energy release rate due to channelling:

$$\mathscr{G}_{ss} = \frac{1}{2}\frac{\sigma^2 h}{\bar{E}_1}\pi g(\alpha, \beta). \tag{8}$$

Numerical results

Table 2 gives values of $f(\alpha, \beta)$, $g(\alpha, \beta)$ and $\delta^*(\alpha, \beta)$ as a function of α for the fully cracked film problem. These values are also plotted in Figs 4, 5 and 6. As detailed in the Introduction, α can vary from -1 to $+1$ and in this paper β is restricted to the practical limits of $\beta = 0$ and $\beta = \alpha/4$. The definition of α given in (1) and the designation of the film as material 1 means that for a film that is stiff relative to the substrate, α is positive and for a compliant film α is negative.

The results plotted in Fig. 4 show that $f(\alpha, \beta)$ decreases as film stiffness increases. Values for f are approximately independent of β for positive α values (stiff film). There is a relatively strong β dependence for the negative α values, however. The results plotted in Fig. 5 show that $g(\alpha, \beta)$ (and thus the likelihood for channelling to occur) increases as film stiffness increases. The dependence of g on β is weak over the full range of α. In Fig. 6, the plot of $\delta^*(\alpha, \beta)$ as a function of α shows that δ^* exhibits characteristics that are essentially identical to those of g. Values for δ^* increase with the relative stiffness of the film and δ^* shows little dependence on β within the practical limits of $\beta = 0$ and $\beta = \alpha/4$.

3. PARTIALLY CRACKED FILM PROBLEM

Problem description and analysis

Because the crack tip is fully within the film, the partially cracked film problem exhibits the $r^{1/2}$ stress singularity associated with classical fracture mechanics problems. Thus, the classical definition of stress intensity factor is used, with

$$K_I \equiv \lim_{y \to 0^-} [\sqrt{-2\pi y}\sigma_{xx}(0, y)]. \tag{9}$$

For the partially cracked film problem, the following two dimensionless quantities analogous to f and g for the fully cracked film problem are defined:

$$F\left(\alpha, \beta, \frac{a}{h}\right) = \frac{K_I}{\sigma(\pi h)^{1/2}}, \quad G\left(\alpha, \beta, \frac{a}{h}\right) = \frac{\int_0^a \delta(y)\,dy}{\pi\frac{\sigma}{\bar{E}_1}ah}. \tag{10}$$

Comparison with (5) shows that as a/h approaches 1, $G(\alpha, \beta, a/h)$ must approach $g(\alpha, \beta)$;

Table 2. f, g and δ^* as a function of α (fully cracked film problem) for $\beta = 0$ and $\beta = \alpha/4$

					$f(\alpha, \beta)$ Compliant film						
α	−0.99	−0.95	−0.90	−0.80	−0.70	−0.60	−0.50	−0.40	−0.30	−0.20	−0.10
$\beta = 0$	1.780	1.760	1.734	1.680	1.623	1.563	1.500	1.432	1.361	1.285	1.205
$\beta = \alpha/4$	3.206	3.047	2.866	2.549	2.280	2.050	1.849	1.672	1.513	1.371	1.241
					$f(\alpha, \beta)$ Stiff film						
α	0.10	0.20	0.30	0.40	0.50	0.60	0.70	0.80	0.90	0.95	0.99
$\beta = 0$	1.034	0.9427	0.8486	0.7522	0.6543	0.5557	0.4566	0.3562	0.2496	0.1874	0.1008
$\beta = \alpha/4$	1.011	0.9067	0.8083	0.7142	0.6233	0.5343	0.4456	0.3546	0.2545	0.1935	0.1074
					$g(\alpha, \beta)$ Compliant film						
α	−0.99	−0.95	−0.90	−0.80	−0.70	−0.60	−0.50	−0.40	−0.30	−0.20	−0.10
$\beta = 0$	0.8153	0.8257	0.8393	0.8684	0.9002	0.9352	0.9740	1.017	1.066	1.121	1.184
$\beta = \alpha/4$	0.7117	0.7254	0.7431	0.7805	0.8212	0.8654	0.9140	0.9676	1.027	1.094	1.170
					$g(\alpha, \beta)$ Stiff film						
α	0.10	0.20	0.30	0.40	0.50	0.60	0.70	0.80	0.90	0.95	0.99
$\beta = 0$	1.344	1.448	1.576	1.737	1.949	2.245	2.692	3.479	5.400	8.430	22.68
$\beta = \alpha/4$	1.360	1.481	1.628	1.813	2.052	2.382	2.876	3.730	5.775	8.940	23.83
					$\delta^*(\alpha, \beta)$ Compliant film						
α	−0.99	−0.95	−0.90	−0.80	−0.70	−0.60	−0.50	−0.40	−0.30	−0.20	−0.10
$\beta = 0$	3.895	3.940	4.000	4.127	4.266	4.419	4.588	4.776	4.988	5.227	5.501
$\beta = \alpha/4$	3.441	3.501	3.578	3.741	3.917	4.110	4.322	4.555	4.815	5.107	5.438
					$\delta^*(\alpha, \beta)$ Stiff film						
α	0.10	0.20	0.30	0.40	0.50	0.60	0.70	0.80	0.90	0.95	0.99
$\beta = 0$	6.190	6.636	7.182	7.870	8.770	10.01	11.89	15.13	22.89	34.71	87.48
$\beta = \alpha/4$	6.261	6.786	7.423	8.218	9.249	10.66	12.75	16.34	24.75	37.32	93.14

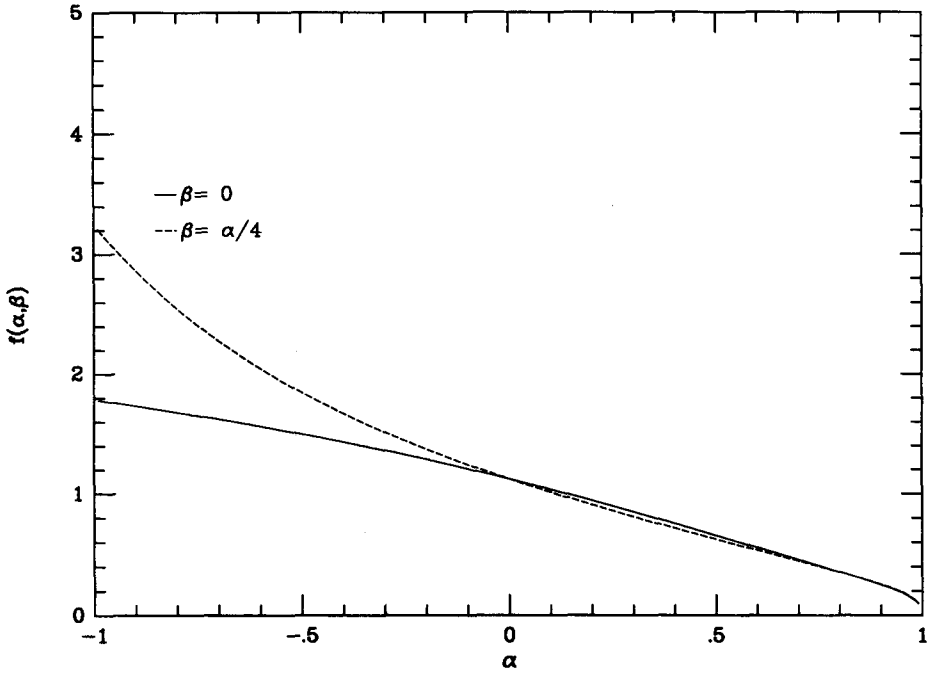

Fig. 4. Plot of $f(\alpha, \beta)$ vs α for $\beta = 0$ and $\beta = \alpha/4$ for the fully cracked film problem.

however, due to the different stress singularities, $F(\alpha, \beta, a/h)$ does not in general approach $f(\alpha, \beta)$. In the absence of elastic mismatch, $F(0, 0, a/h) = 1.1215\sqrt{a/h}$ and $G(0, 0, a/h) = (1.1215)^2(a/h)$.

For a partially cracked film, two modes of crack extension are possible. The 2-D plane strain crack can extend toward the interface and the 3-D crack can channel across the film. For the channelling crack, a steady-state argument analogous to that made for the fully cracked problem gives that the total work release per unit crack extension must equal ΔE, where

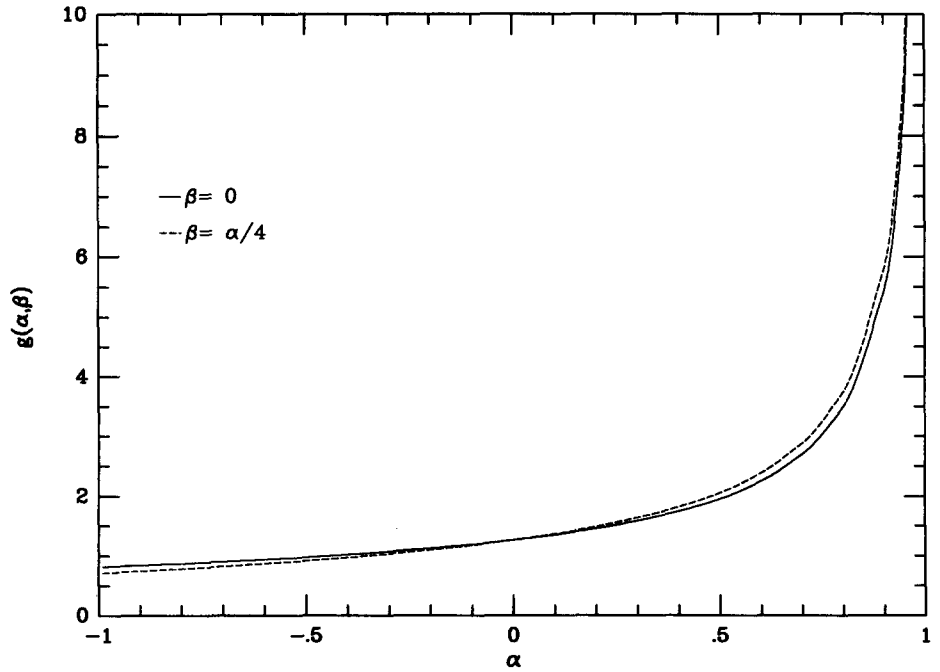

Fig. 5. Plot of $g(\alpha, \beta)$ vs α for $\beta = 0$ and $\beta = \alpha/4$ for the fully cracked film problem.

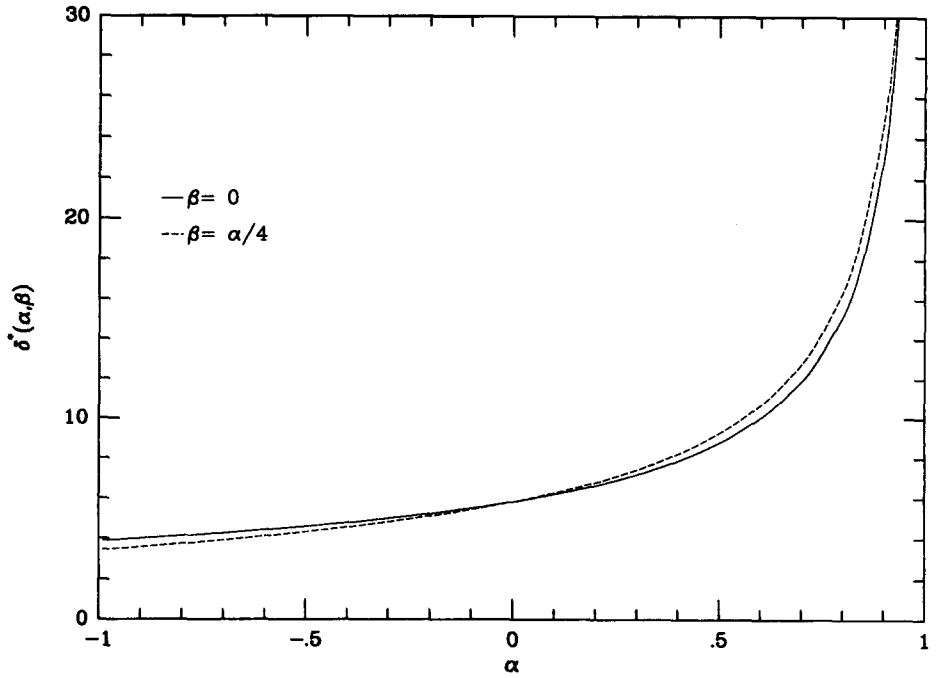

Fig. 6. Plot of $\delta^*(\alpha, \beta)$ vs α for $\beta = 0$ and $\beta = \alpha/4$ for the fully cracked film problem.

$$\Delta E = \frac{\sigma}{2}\int_0^a \delta(y)\,dy, \tag{11}$$

and now the extending crack front has a length a instead of h. The steady-state energy release rate of the channelling crack is thus given by $\mathcal{G}_{ss} = \Delta E/a$. Using the definition of $G(\alpha, \beta, a/h)$ yields the following equation for $\mathcal{G}_{ss}$:

$$\mathcal{G}_{ss} = \frac{1}{2}\frac{\sigma^2 h}{\bar{E}_1}\pi G\left(\alpha, \beta, \frac{a}{h}\right). \tag{12}$$

It is shown in the next section on numerical results that an existing flaw part-way through a film that is compliant with respect to the substrate will not propagate all the way to the film/substrate interface. In such cases, the 2-D plane strain crack will grow to a length, a, which is less than the film thickness, h, and (12) can be applied to predict whether 3-D channelling will occur.

Numerical results

Figures 7 and 8 provide plots of $F(a, \beta, a/h)$ as a function of a/h for select values of α and for $\beta = 0$ (Fig. 7) and $\beta = \alpha/4$ (Fig. 8). Although it is not obvious to the eye, there can, in general, be a β-dependence in the results which is significant. The trends in K_I (and thus F) as a function of a/h have been explored previously in the literature by Gecit (1979) and Lu and Erdogan (1983b). Regardless of the values of α and β, $F(\alpha, \beta, a/h)$ approaches the homogeneous half plane value of $1.1215\sqrt{a/h}$ as a/h approaches zero. For films that are compliant with respect to the substrate, a maximum in $F(\alpha, \beta, a/h)$ occurs within $0 < a/h < 1$ and F approaches zero as a/h approaches 1. Thus, given a flaw of a certain size in a compliant film, once the critical stress intensity factor is reached, the crack will grow toward the interface until $K_I = \sigma(\pi h)^{1/2}F$ becomes less than K_{Ic}, at a value of a/h close to, but less than, 1. In principle, then, an existing flaw in a film that is compliant with respect to the substrate will never propagate all the way to the interface. For films that are stiff relative to the substrate, F approaches infinity as a/h approaches 1. As a result, for a given flaw size in a

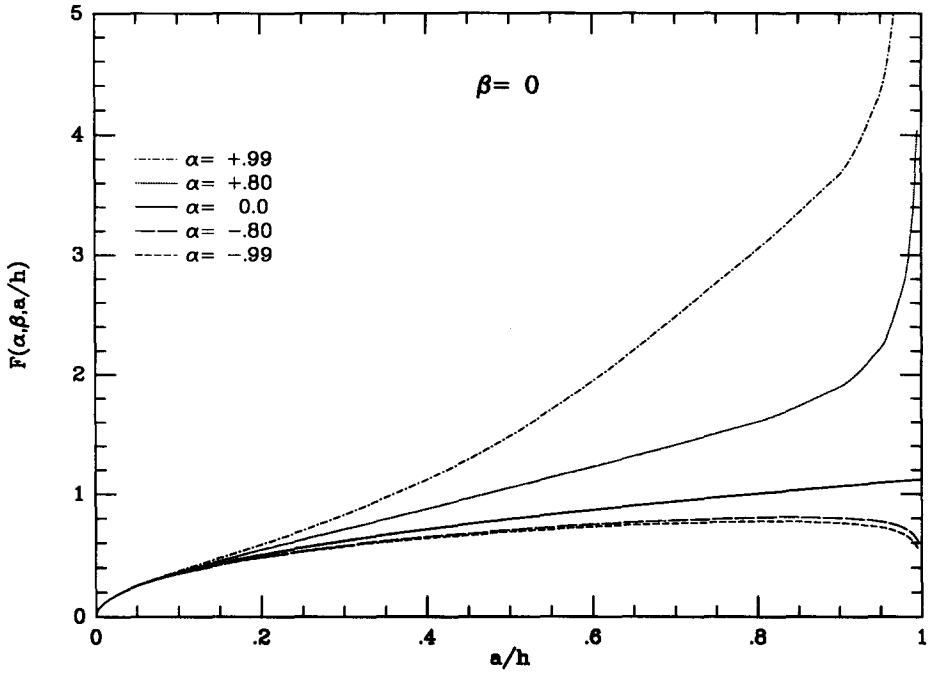

Fig. 7. Plot of $F(\alpha, \beta, a/h)$ vs a/h (partially cracked film problem) for $\beta = 0$.

stiff film, once K_{Ic} is reached the crack will propagate all the way to the interface, resulting in the fully cracked film problem.

Figures 9 and 10 offer plots of $G(\alpha, \beta, a/h)$ analogous to the plots of F in Figs 7 and 8. The values for G generally exhibit a weaker β-dependence than the F values. As a/h approaches zero, $G(\alpha, \beta, a/h)$ approaches the homogeneous half plane value of $(1.1215)^2(a/h)$ for all values of α and β. The plots show that compliant films exhibit a shallow maximum in G near $a/h = 1$. For stiff films, the maximum in G is at $a/h = 1$.

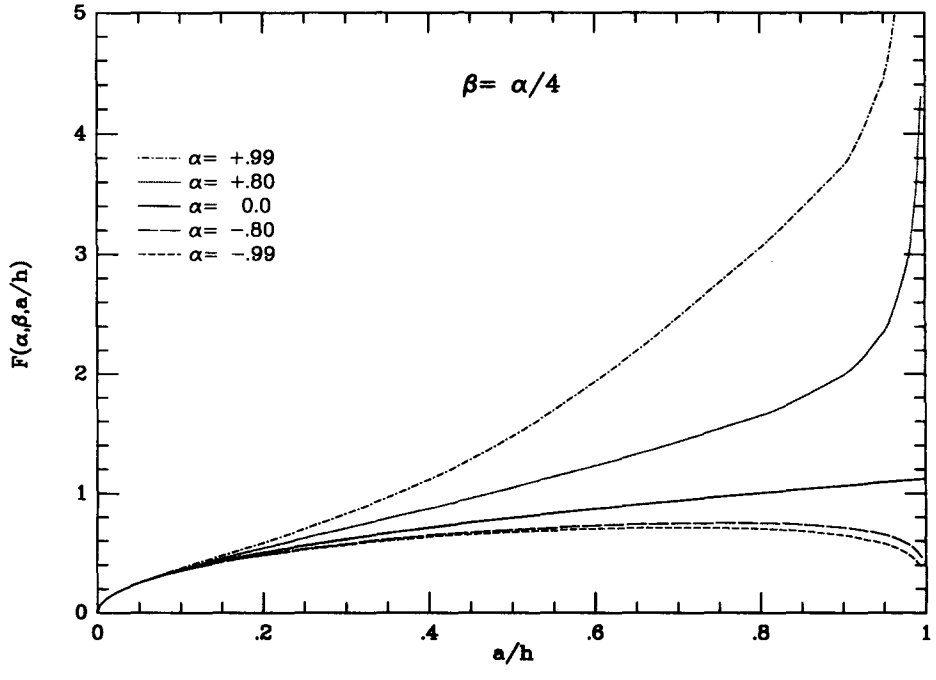

Fig. 8. Plot of $F(\alpha, \beta, a/h)$ vs a/h (partially cracked film problem) for $\beta = \alpha/4$.

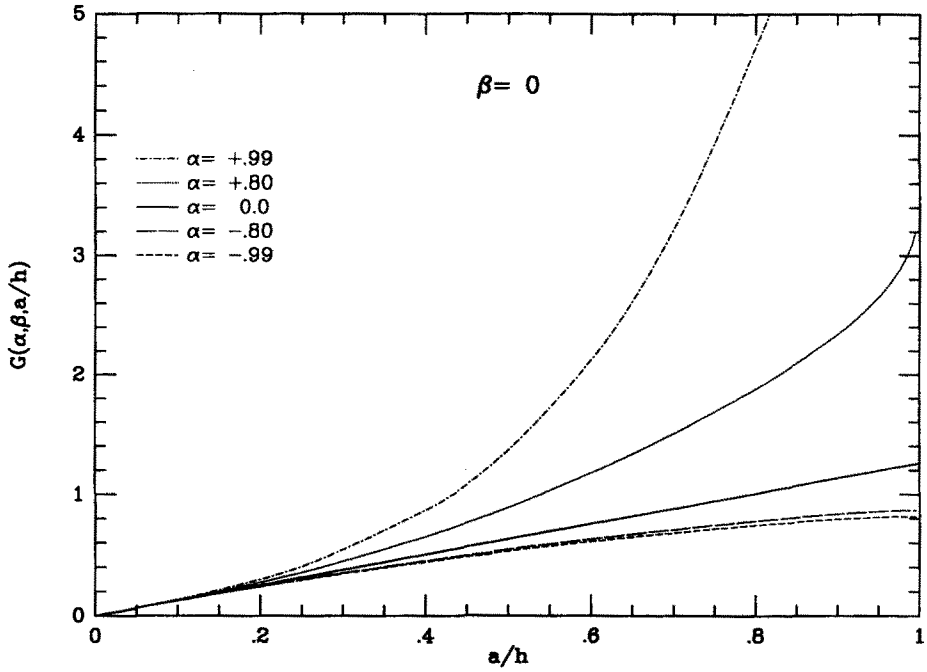

Fig. 9. Plot of $G(\alpha, \beta, a/h)$ vs a/h (partially cracked film problem) for $\beta = 0$.

Regardless of the stiffness of the film relative to the substrate, $G(\alpha, \beta, a/h)$ approaches $g(\alpha, \beta)$ as a/h approaches 1.

For a given compliant film/stiff substrate combination, the maximum values of F and G are of particular interest as design parameters. If K_{Ic} for the film is greater than K_{Imax} calculated from F_{max}, then no extension of the 2-D plane strain crack toward the interface is possible, irrespective of the initial flaw length. Similarly, if $\mathcal{G}_{Ic}$ for the film is greater than $\mathcal{G}_{ss(max)}$ calculated from G_{max}, then no channelling can occur. Approximate formulas for F

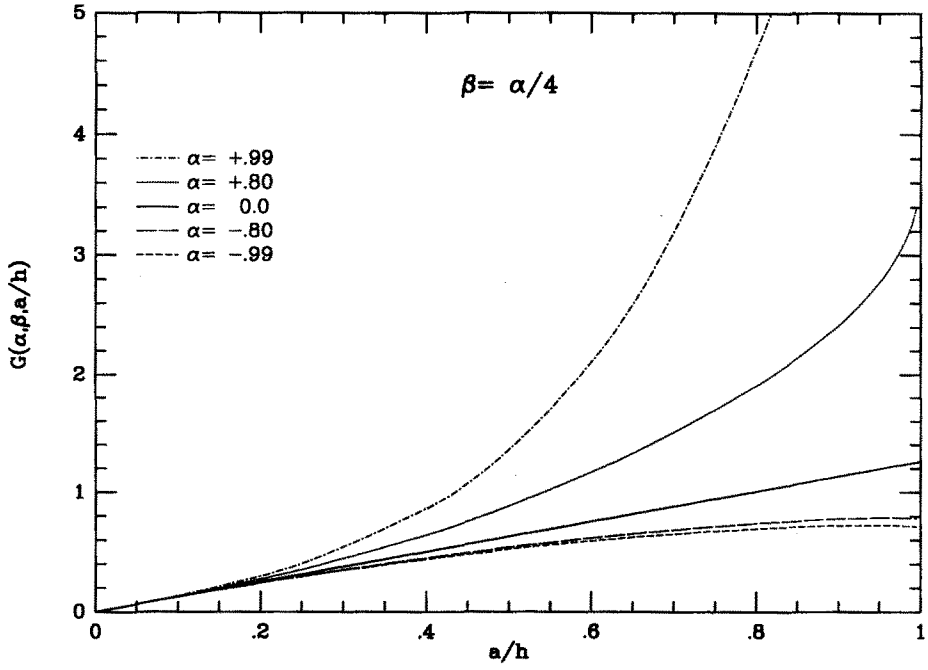

Fig. 10. Plot of $G(\alpha, \beta, a/h)$ vs a/h (partially cracked film problem) for $\beta = \alpha/4$.

and G are given in the next section. An important relation exists, however, coupling F and G at the location where G is a maximum.

Using the fact that $\mathcal{G}_{ss} = \Delta E/a$ for the partially cracked film problem, and using a relation analogous to that given for the fully cracked problem in (7), yields the following relation for $\mathcal{G}_{ss}$:

$$\mathcal{G}_{ss} = \frac{1}{a}\int_0^a \mathcal{G}_{ps}\, da, \tag{13}$$

where the notation $\mathcal{G}_{ps}$ has been used in place of $\mathcal{G}$ to emphasize that it is the energy release rate of the 2-D plane strain crack. Taking the derivative of (13) with respect to a gives

$$\frac{d\mathcal{G}_{ss}}{da} = \frac{1}{a}\mathcal{G}_{ps} - \frac{1}{a^2}\int_0^a \mathcal{G}_{ps}\, da = \frac{1}{a}(\mathcal{G}_{ps} - \mathcal{G}_{ss}). \tag{14}$$

Thus, $d\mathcal{G}_{ss}/da = 0$ for $\mathcal{G}_{ss}$ equal to $\mathcal{G}_{ps}$, which defines a condition for the location of the maximum of $\mathcal{G}_{ss}$ for the compliant film problem. Setting $\mathcal{G}_{ss}$ equal to $\mathcal{G}_{ps}$ and using the relation between $\mathcal{G}_{ss}$ and $G(\alpha, \beta, \alpha/h)$ in (12), the relation between K_I and $F(\alpha, \beta, a/h)$ in (10), and the fact that $\mathcal{G}_{ps} = K_I^2/\bar{E}_1$, gives that $F^2 = G/2$ at the value of a where $\mathcal{G}_{ss}$ is a maximum. Thus at the value of a/h where $F^2 = G/2$, it must be true that $G(\alpha, \beta, a/h)$ is maximized.

Figure 11 gives a typical plot of normalized values of $\mathcal{G}_{ps}$ calculated from K_I for the plane strain cracking problem and normalized values of $\mathcal{G}_{ss}$ for the channelling crack, both versus a/h. The figure delineates the role of the normalized film toughness, $\bar{E}_1\mathcal{G}_{Ic}/\sigma^2 h$, on the likelihood for each type of film crack extension. Whether each type of cracking will actually occur is, in general, dependent on the length of initial flaws in the film. However, if $\bar{E}_1\mathcal{G}_{Ic}/\sigma^2 h$ for the film is above the maximum of the normalized $\mathcal{G}_{ps}$ curve, no crack extension of either kind can occur for any initial flaw size. For a value of $\bar{E}_1\mathcal{G}_{Ic}/\sigma^2 h$ for the film between the maximum of the $\mathcal{G}_{ps}$ curve and the maximum of the $\mathcal{G}_{ss}$ curve (located where the curves intersect and $F^2 = G/2$), extension of a plane strain crack toward the interface can occur, but channelling cannot. If the normalized $\mathcal{G}_{Ic}$ of the film is below the maximum

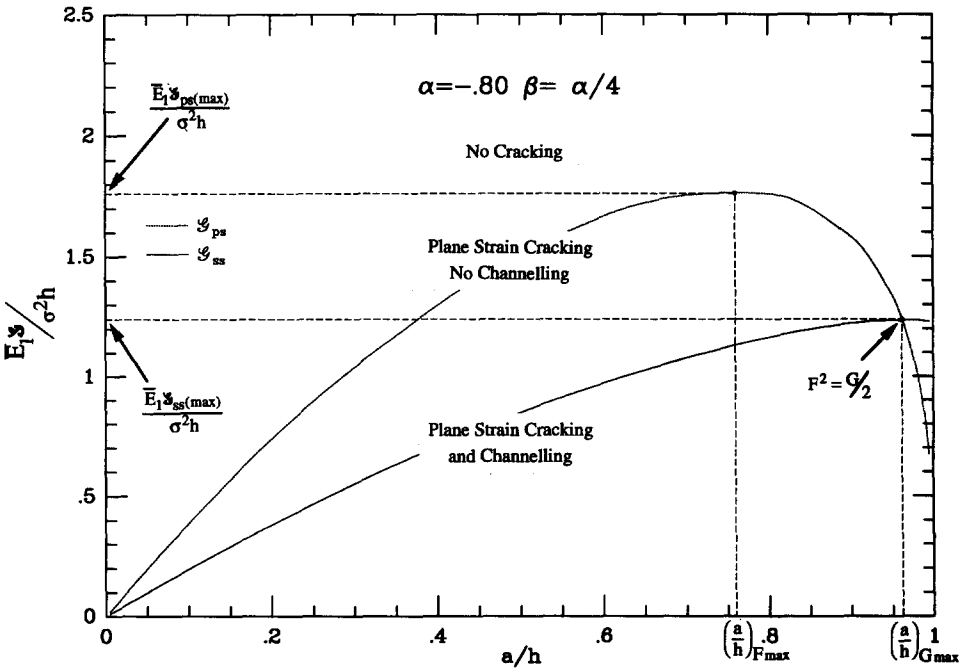

Fig. 11. Plot of regions of plane strain cracking and steady-state channelling vs a/h for $\alpha = -0.80$, $\beta = \alpha/4$.

of the $\mathcal{G}_{ss}$ curve, then both types of cracking can occur. If plane strain crack extension is initiated, it will continue until $\mathcal{G}_{ps}$ falls below $\mathcal{G}_{Ic}$, at the value of a/h determined by the intersection of the normalized toughness with the right-hand portion of the $\mathcal{G}_{ps}$ curve. Because $\mathcal{G}_{ss} > \mathcal{G}_{ps}$ for $a/h > a/h|_{G_{max}}$, if channelling is initiated, it will proceed until the crack runs through the entire film or until a boundary is reached.

Approximate formulas

Presentation of the numerical results for F and G in a form that fully maps out their dependence on the three parameters α, β and a/h is difficult. Thus, approximate formulas are proposed here for the dimensionless quantities $F(\alpha, \beta, a/h)$ and $G(\alpha, \beta, a/h)$ to allow easier prediction of thin film cracking behavior based on the solution results. The approximation for $F(\alpha, \beta, a/h)$ elaborates upon a suggestion to the author by Z. Suo. It is

$$F\left(\alpha, \beta, \frac{a}{h}\right) = \frac{K_I}{\sigma\sqrt{\pi h}} = 1.1215\left(\frac{a}{h}\right)^{1/2}\left(1-\frac{a}{h}\right)^{(1/2)-s}\left(1+\lambda\frac{a}{h}\right), \tag{15}$$

where the α and β dependence is through the Zak–Williams singularity s and the fitting parameter λ. The formula for F is defined so as to satisfy the following criteria:

(1) F must approach $1.1215(a/h)^{1/2}$ for the case of no elastic mismatch ($s = 1/2$).
(2) F must approach $1.1215(a/h)^{1/2}$ as a/h approaches 0.
(3) F must have a (1/2-s) singularity as a/h approaches 1.

Criterion 3 is arrived at by the following argument. First, the stress intensity factor for the fully cracked film problem is of the form $K_I^* \propto \sigma h^s$. Second, the stress intensity factor for the partially cracked film problem must be of the form $K_I \propto \sigma(\text{length})^{1/2}$. For the case of the crack tip approaching the interface, with $(h-a) \ll h$, an asymptotic problem for K_I can be posed such that K_I must depend linearly on K_I^* and where the only length parameter is $(h-a)$. From the dimensionality of K_I^* and K_I it follows that K_I is proportional to $K_I^*(h-a)^{(1/2-s)}$ as a approaches h. Thus

$$\frac{K_I}{\sigma\sqrt{h}} \propto \left(1-\frac{a}{h}\right)^{(1/2-s)}$$

as a/h approaches 1.

The parameter $\lambda(\alpha, \beta)$ in (15) is a fitting parameter that is used to match the approximate formula to numerical values of F from the solution at $a/h = 0.98$. The idea behind using the parameter λ is to increase the accuracy of the formula by matching the solution near $a/h = 1$, in a way similar to the way it is matched at $a/h = 0$. Criterion 1 requires that $\lambda = 0$ for the case of no elastic mismatch. For compliant film problems, the approximation for F given in (15) exhibits a maximum at

$$2\left(\frac{a}{h}\right)_{F_{max}} = -b + \sqrt{b^2 + \frac{4}{4\lambda - 2s\lambda}}, \tag{16}$$

where

$$b = \frac{2-2s-3\lambda}{4\lambda-2s\lambda}. \tag{17}$$

An approximate formula for $G(\alpha, \beta, a/h)$ is obtained by using the relation between $\mathcal{G}_{ss}$ and $\mathcal{G}_{ps}$ given in (13), along with the definition of F and the fact that $\mathcal{G}_{ps} = K_I^2/\bar{E}_1$. A change of variables produces a polynomial expression that can be integrated by hand to give the following formula:

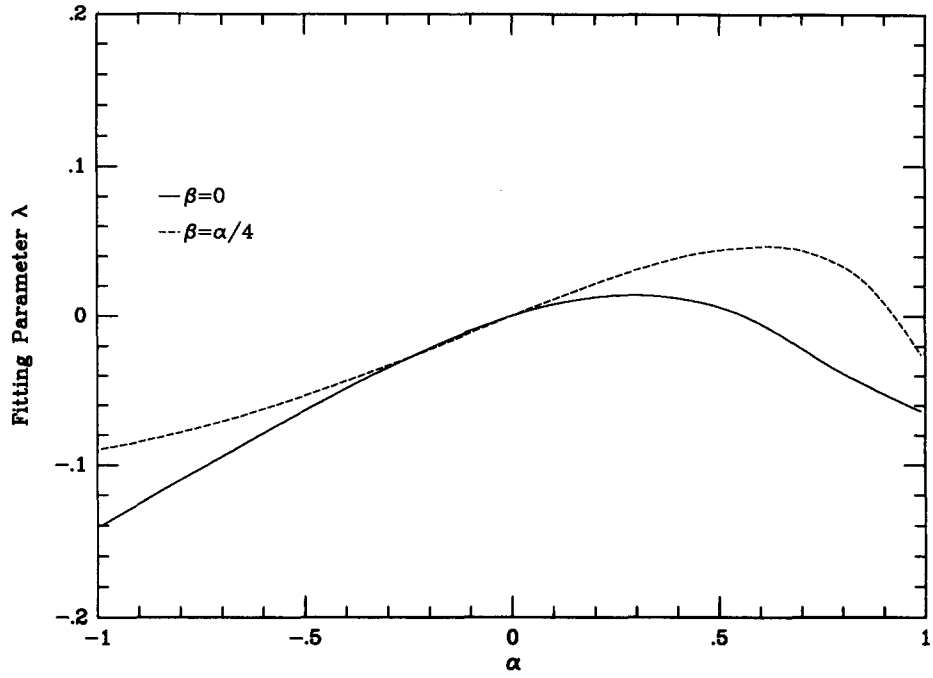

Fig. 12. Plot of approximate formula fitting parameter λ vs α for $\beta = 0$ and $\beta = \alpha/4$.

$$G\left(\alpha,\beta,\frac{a}{h}\right) = -\frac{2h}{a}(1.1215)^2\left[b^{2-2s}\left(\frac{1+2\lambda+\lambda^2}{2-2s} - \frac{(1+4\lambda+3\lambda^2)b}{3-2s} + \frac{(2\lambda+3\lambda^2)b^2}{4-2s} - \frac{\lambda^2 b^3}{5-2s}\right)\right]_{b=1}^{b=1-(a/h)} \quad (18)$$

Figure 12 provides a plot of λ vs α for the two cases of $\beta = 0$ and $\beta = \alpha/4$. Numerical values are provided in Table 3. For the convenience of the reader, analogous data for s is provided in Table 1 and plotted in Fig. 2. These plots and tables can be used in conjunction with (15) and (18) to obtain approximate values of F and G for the partially cracked film problem. As indicated in Fig. 12, λ is typically small in magnitude and equal to zero for the case of identical film and substrate materials. Reasonable estimates can, in fact, be obtained for F and G by simply taking $\lambda = 0$.

Figures 13 and 14 provide comparisons of the approximate formulas for F and G with fully accurate numerical values which were plotted in Figs 8 and 10. In the figures, data points are from the solution and lines are generated from the approximate formulas for F and G. The plots clearly show that the approximate formulae are very accurate for the compliant film cases. For example, the maximum error in the formula for F for the case of $\alpha = -0.99$, $\beta = -0.2475$ (the bottom line in Fig. 13) is less than 2 percent. The formulae can thus serve as powerful, simple representations of the dependence of F and G on α, β, and a/h for compliant film problems. The formulae for F and G show some disagreement with the solution results for problems where the film is much stiffer than the substrate, however, Although the approximate formula for F gives good agreement with the actual

Table 3. Fitting parameter, λ, as a function of α for $\beta = 0$ and $\beta = \alpha/4$

α	−0.99	−0.80	−0.60	−0.40	−0.20	0.0
$\beta = 0$	−0.1399	−0.1103	−0.0790	−0.0488	−0.0215	0.0
$\beta = \alpha/4$	−0.0894	−0.0784	−0.0627	−0.0437	−0.0224	0.0
α	0.20	0.40	0.60	0.80	0.99	
$\beta = 0$	0.0125	0.0119	−0.0049	−0.0383	−0.0638	
$\beta = \alpha/4$	0.0215	0.0389	0.0465	0.0335	−0.0257	

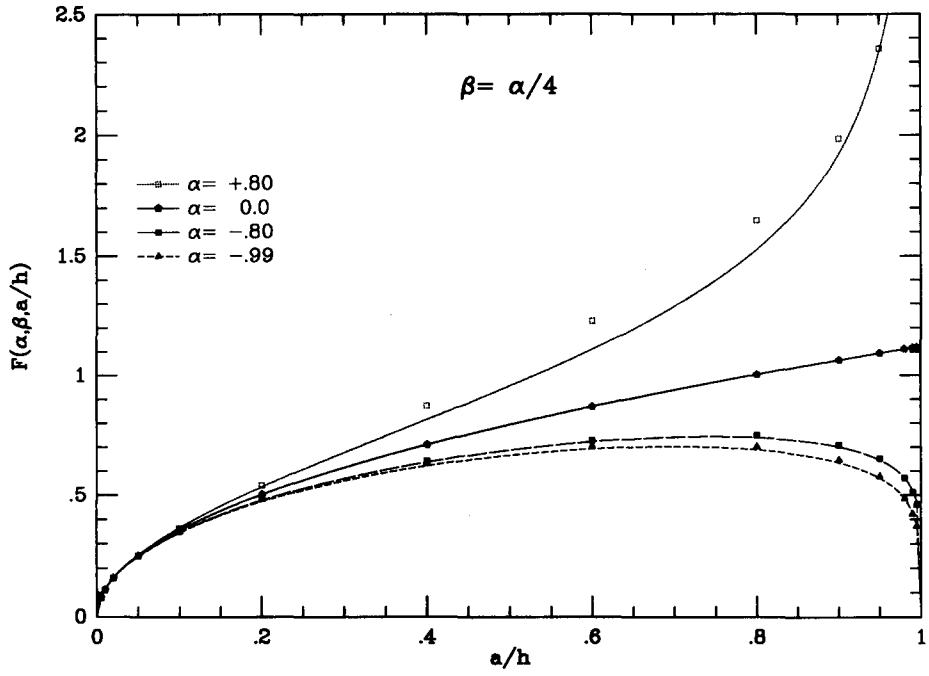

Fig. 13. Comparison of approximate formula for F and numerical solution data for $\beta = \alpha/4$.

values of F near $a/h = 0$ and $a/h = 1$, the approximation underestimates F near $0.40 \leqslant a/h \leqslant 0.80$. Values of G are thus underestimated for $a/h \geqslant 0.40$. Care should thus be taken in using the formulas for F and G for stiff problems within these ranges of a/h.

4. APPLICATIONS OF THE RESULTS

Predicting thin film cracking behavior

The results for the partially cracked film problem show that a flaw of a given size in a film under residual tension will begin to propagate toward the interface when the stress

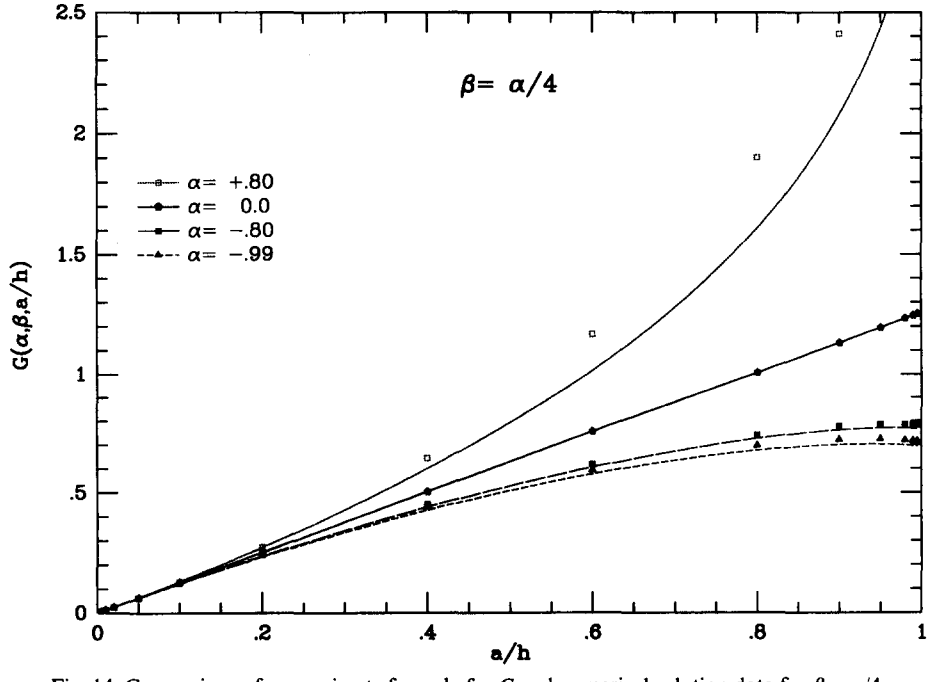

Fig. 14. Comparison of approximate formula for G and numerical solution data for $\beta = \alpha/4$.

intensity factor, K_I, calculated from $F(\alpha, \beta, a/h)$ is greater than the K_{Ic} of the film. When this happens, the crack may or may not propagate all the way to the interface depending on whether the film is stiff or compliant with respect to the substrate. At the same time, for a given crack length there is a corresponding value of $G(\alpha, \beta, a/h)$ or $g(\alpha, \beta)$ that is related to the energy release rate of a steady-state crack channelling across the film, $\mathcal{G}_{ss}$. When $\mathcal{G}_{ss}$ is greater than the $\mathcal{G}_{Ic}$ of the film, crack channelling across the film will occur.

Hutchinson and Suo (1990) explore in detail these matters and others related to the cracking of thin films in tension. Figure 15 gives an illustration of how the results and approximate formulas presented in this study can be applied by a designer to determine what type of cracking can or cannot occur for a given film/substrate combination, film thickness, h, and stress σ. Normalized values of $\mathcal{G}_{ps}$ and $\mathcal{G}_{ss}$ are plotted in Fig. 15 as a function of α, with $\beta = \alpha/4$, for comparison with normalized values of $\mathcal{G}_{Ic}$. An initial flaw size of $a/h = 0.80$ was used to calculate the plane strain energy release rate values. For stiff film cases, as long as initial flaws are smaller than $0.80h$, the plotted $\mathcal{G}_{ps}$ values represent upper bounds to the actual values. For compliant film cases, because the maximum of $\mathcal{G}_{ps}$ typically occurs near $a/h = 0.80$ (see Fig. 11), use of an initial flaw size of $a/h = 0.80$ to calculate $\mathcal{G}_{ps}$ values roughly corresponds to the most severe flaw possible. Similarly, $g(\alpha, \beta)$ for the fully cracked film problem was used to calculate the energy release rates for steady-state channelling. For a stiff film, the maximum value of $\mathcal{G}_{ss}$ occurs at $a/h = 1$. As illustrated in Fig. 11, for a compliant film the maximum in $\mathcal{G}_{ss}$ occurs very near $a/h = 1$. Because compliant film $\mathcal{G}_{ss}$ curves are very flat in the region near $a/h = 1$, use of $g(\alpha, \beta)$ to calculate $\mathcal{G}_{ss}$ yields a value that is very close to the maximum. In Fig. 15, for a value of normalized film toughness, $\bar{E}_1 \mathcal{G}_{Ic}/\sigma^2 h$, which is above both curves, no crack extension can occur. For normalized toughnesses in the region between the curves, only plane strain crack extension toward the interface can occur. In the region below both curves, both plane strain extension and steady-state crack channelling can occur.

Curvature change due to cracking of a thin bonded film

The quantity $g(\alpha, \beta)$ for the fully cracked film problem is used here to calculate the change in curvature of a film/substrate wafer when cracking occurs in the film. The change in angular rotation of the wafer ends due to the introduction of a single plane strain crack

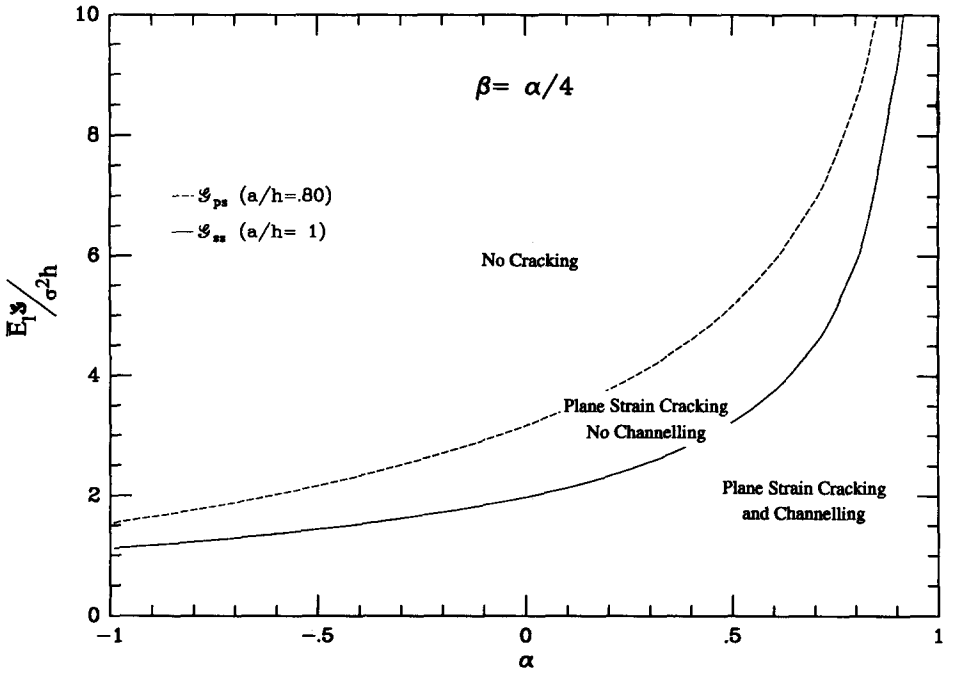

Fig. 15. Regions of plane strain cracking and steady-state channelling vs α for $\beta = \alpha/4$.

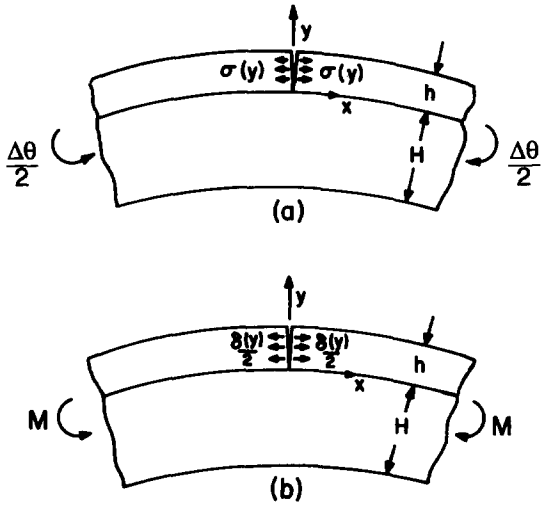

Fig. 16. Reciprocal theorem analysis used to calculate the angular rotation of the film/substrate wafer ends due to cracking in the film.

of length h can be determined using the Reciprocal Theorem analysis illustrated in Fig. 16. The problem to be solved is that of a traction-free crack in a film supporting a tensile stress $\sigma(y)$ prior to introduction of the crack. The equivalent fracture mechanics problem is that of a cracked wafer with pressure $\sigma(y)$ applied to the crack faces (Fig. 16a). The unknown quantity to be solved for is $\Delta\theta$. The auxiliary problem, illustrated in Fig. 16b, is the same cracked wafer subject to a unit bending moment per unit depth, M, with crack opening displacements, $\delta(y)$. Reciprocity requires that

$$M^{(2)}\Delta\theta^{(1)} = \int_0^h \sigma(y)^{(1)}\delta(y)^{(2)}\,dy. \tag{19}$$

If the film is thin with respect to the substrate ($h \ll H$), the following assumptions are valid.

(1) The stress in the film, σ, is uniform. Thus σ for problem 1 is y-independent.
(2) For problem 2, the stress in the film prior to introduction of the crack is

$$\sigma^{(2)} = \frac{6M^{(2)}}{H^2}\frac{\bar{E}_1}{\bar{E}_2}. \tag{20}$$

(3) For problem 2, $\delta(y)$ is equal to the crack opening displacement for a film supporting a stress $\sigma^{(2)}$ and attached to an infinitely deep substrate (to lowest order in h/H).

For the second assumption to be true, the film must not contribute significantly to the bending stiffness of the film/substrate wafer ($E_1h/E_2H \ll 1$). Substituting the above into (19) and using the definition of $g(\alpha, \beta)$ results in the following formula for $\Delta\theta$, the change in angular rotation of the film/substrate ends due to the formation of a single crack:

$$\Delta\theta = 6\pi\frac{\sigma}{\bar{E}_2}\left(\frac{h}{H}\right)^2 g(\alpha, \beta). \tag{21}$$

This formula can also be used to estimate the change of curvature of the film/substrate wafer due to the formation of multiple cracks, as long as the cracks are far enough apart to neglect interaction. Related calculations by Thouless (1990) which neglect elastic mismatch suggest that interaction only becomes significant when the crack spacing is less than 8 film thicknesses. If s_0 is designated as the average spacing between cracks in the film, then the change in curvature, $\Delta\kappa$, of the wafer due to the formation of multiple cracks is given by

$$\Delta\kappa = 6\pi\frac{\sigma}{\bar{E}_2 s_0}\left(\frac{h}{H}\right)^2 g(\alpha, \beta). \tag{22}$$

The formulae given in (21) and (22) have been derived assuming that an existing flaw or flaws in the film will propagate all the way to the film/substrate interface, even though in theory this can only happen in a film which is stiff with respect to the substrate. However, the results for $F(\alpha, \beta, a/h)$ for the partially cracked film show that cracks in films which are compliant with respect to the substrate will *almost* extend to meet the interface. This fact and the fact that the plots of $G(\alpha, \beta, a/h)$ for compliant films are very flat near $a/h = 1$ indicate that no significant error is introduced by assuming all cracks in the film extend to the interface. The relation in (22) has been derived with a specific application in mind. An established experimental technique for estimating residual stresses in bonded thin films involves measuring the resulting change in curvature in the substrate due to application of the film. A concise description of the method, which assumes that no film cracking has occurred, is given by Nix (1989). Unfortunately, in many cases the thin bonded film does crack due to the residual stress. In such cases, (22) can be used to estimate the effect of film cracking on the measured curvature change. No other method of accounting for film cracking is currently available to experimenters using the curvature method to measure residual stress in thin films bonded dissimilar elastic substrates. In recent work, however, Thouless *et al.* (1991) have developed, on conjunction with the analysis presented here, relations for the curvature change for interacting cracks (i.e. spacing less than 8 film thicknesses) for the case of no elastic mismatch.

5. CONCLUSIONS

Solutions have been obtained for two elastic fracture mechanics problems that have been used to characterize the cracking of thin films bonded to thick substrate materials. A dimensionless plane strain stress intensity factor and a dimensionless integral of the crack opening displacement have been extracted from both solutions. The integral of the crack opening displacement has been related to the steady-state energy release rate for crack channelling across the film for both problems studied. To facilitate comparison of the analysis with experiments, a dimensionless crack opening displacement evaluated at the top of the crack has been extracted from the solution for the fully cracked film problem. Solution results have been presented for both problems and, for the partially cracked film problem, approximate formulae have been given for the dimensionless quantities as a function of the normalized crack length. The approximate formulae are most accurate when the film is compliant with respect to the substrate. Applications of the results and approximate formulae have been detailed. These include the roles of the nondimensional parameters in predicting the cracking of thin films. In addition, the integral of the crack opening displacement for the fully cracked film problem has been related to the change in curvature in a film/substrate wafer due to film cracking. The result is a complete set of solution results and approximate formulae for practical application in understanding the cracking behavior of thin films adhered to thick substrate materials.

Acknowledgements—This work was supported by the DARPA University Research Initiative (Subagreement P.O. #VB38639-0 with the University of California, Santa Barbara, ONR Prime Contract N00014-86-K0753), by NSF Grant MSM-88-12779 and by the Division of Applied Sciences, Harvard University. The author would like to thank John Hutchinson for his advice, input and inspiration throughout this effort and William Nix for motivating the work on calculating curvature changes due to film cracking. The author also gratefully acknowledges the efforts of Zhigang Suo in helping to formulate the approximate formulae presented.

REFERENCES

Civilek, M. B. (1985). Stress intensity factors for a system of cracks in an infinite strip. *Fracture Mechanics: Sixteenth Symposium* (Edited by M. F. Kanninen and A. T. Hopper), ASTM STP 868, 7–26.
Dundurs, J. (1969). Edge-bonded dissimilar orthogonal elastic wedges. *J. Appl. Mech.* **36**, 650–652.
Gecit, M. R. (1979). Fracture of a surface layer bonded to a half space. *Int. J. Engng Sci.* **17**, 287–295.

Hutchinson, J. W. and Suo, Z. (1991). Mixed mode cracking in layered materials. In *Advances in Applied Mechanics* (Edited by J. W. Hutchinson and T. Y. Wu). Vol. 29, pp. 63–191. Academic Press, New York.
Lu, M.-C. and Erdogan, F. (1983a). Stress intensity factors in two bonded elastic layers containing cracks perpendicular to and on the interface—I. Analysis. *Engng Fract. Mech.* **18,** 491–506.
Lu, M.-C. and Erdogan, F. (1983b). Stress intensity factors in two bonded elastic layers containing cracks perpendicular to and on the interface—II. Solution and results. *Engng Fract. Mech.* **18,** 507–528.
Nakamura, T. and Kamath, S. M. (1991). Three-dimensional effects in thin film fracture mechanics. To be published.
Nix, W. D. (1989). Mechanical properties of thin films. *Met Trans A* **20A,** 2217–2245.
Press, W. H., Flannery, B. P., Teukolsky, S. A. and Vetterling, W. T. (1986). *Numerical Recipes The Art of Scientific Computing.* Cambridge University Press, 147–154.
Rice, J. R. (1968). Mathematical analysis in the mechanics of fracture. In *Fracture, An Advanced Treatise,* II (Edited by H. Liebowitz), pp. 191–311. Academic Press, New York.
Suga, T., Elssner, E. and Schmander, S. (1988). Composite parameters and mechanical compatibility of material joints. *J. Comp. Mater.* **22,** 917–934.
Suo, Z. and Hutchinson, J. W. (1989). Steady-state cracking in brittle substrates beneath adherent films. *Int. J. Solids Structures* **25,** 1337–1353.
Suo, Z. and Hutchinson, J. W. (1990). Interface crack between two elastic layers. *Int. J. Fracture* **43,** 1–18.
Tada, H., Paris, P. and Irwin, G. (1985). *The Stress Analysis of Cracks Handbook* (2nd Edn). Paris Productions, Inc., St. Louis, 8.1a.
Thouless, M. D. (1990). Crack spacing in brittle films on elastic substrates. *J. Am. Ceram. Soc.* **73,** 2144–2146.
Thouless, M. D., Olsson, E. and Gupta, A. (1991). Cracking of brittle films on elastic substrates. *Acta Metall. et Mater.* (to be published).
Zak, A. R. and Williams, M. L. (1963). Crack point singularities at a bimaterial interface. *J. Appl. Mech.* **30,** 142–143.

APPENDIX: PROBLEM SOLUTION

Solution procedure

Rice (1968) gives a general description of the dislocation formulation used by Civilek (1985) and Suo and Hutchinson (1989, 1990) and used in this study to solve the fully cracked and partially cracked film problems. Because of the similarity of the solution procedure used here with that detailed in previous work, the following is only a brief outline of the steps involved in solving the two cracked film problems. Figure 17 illustrates the superposition scheme used to solve the fully cracked film and partially cracked film problems. Figure 17c shows the fundamental problem that must be modelled, that of a semi-infinite bimaterial with a single edge dislocation at $(x = 0, y = \xi)$ with Burgers vector of magnitude b in the positive x direction. This problem is constructed by superimposing the problems of Figs 17a,b. Figure 17a shows an infinite bimaterial with a single dislocation in material 1 located at $(x = 0, y = \xi)$. The stresses in each material are a function of the material parameters α and β and the coordinates x, y and ξ. Methods of obtaining these stresses via complex variable analyses are outlined by Suo and Hutchinson (1989, 1990). A real variable analysis can also be applied, using methods similar to those of Civilek (1985). Figure 17b shows a semi-infinite bimaterial with no dislocation, but with tractions applied along its top boundary. The Fourier transform method for obtaining the solution for the problem in Fig. 17b is outlined by Civilek (1985) and Suo and Hutchinson (1989, 1990). If these tractions are set equal to the negative of the tractions along $y = h$ for the problem in Fig. 17a, then the result upon superposition is the problem in Fig. 17c, with a free surface along $y = h$.

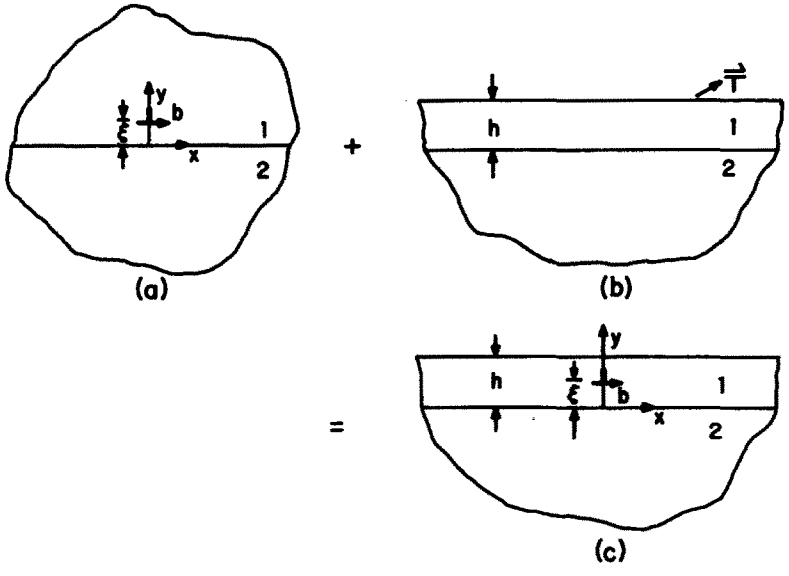

Fig. 17. Superposition scheme used to solve the cracked film problems.

Once the problem of a single dislocation in a semi-infinite bimaterial is constructed, the crack problem is modelled as a string of dislocations along the crack line, with a continuously variable Burgers vector magnitude $b(\xi)$. The crack face traction boundary condition for the particular problems at hand is that $\sigma_{xx}(x=0, y) = -\sigma$ where σ is a uniform pressure load applied to the crack faces. This loading configuration is, from a fracture mechanics standpoint, equivalent to a traction-free crack in a film supporting a uniform tensile stress σ prior to introduction of the crack. The crack face traction boundary condition is enforced by integration of the stresses along $x = 0$ with respect to the dislocation variable, ξ. The resulting integral equation takes the form

$$\sigma_{xx}(0, y) = -\sigma = \frac{-\mu_1}{2\pi(1-\nu_1)} \int_{a_0}^{h} b(\xi)\left[\frac{1}{(y-\xi)} + F_1(0, y, \xi) + F_2(0, y, \xi)\right] d\xi, \tag{A1}$$

where $a_0 = 0$ for the fully cracked film problem and $a_0 = (h-a)$ for the partially cracked film problem with crack length a. The first term, which is integrated in the Cauchy principal value sense, is from the dislocation solution for the problem in Fig. 17a. $F_1(x, y, \xi)$ and $F_2(x, y, \xi)$ are known kernel functions extracted from the solutions of the problems illustrated in Fig. 17a and Fig. 17b, respectively.

The unknown $b(\xi)$ is solved for by first introducing a change of variable

$$t = \frac{2(\xi - a_0)}{(h-a_0)} - 1, \tag{A2}$$

where t can vary from -1 to $+1$. Then $b(t)$ is expressed as a Chebyshev polynomial series with N unknown coefficients, C_k:

$$b(t) = \frac{1}{(t+1)^s} \sum_{k=1}^{N} C_k T_{k-1}(t), \tag{A3}$$

where s is the stress singularity exponent which satisfies (3) for the fully cracked film problem and which equals 1/2 for the partially cracked film problem. The $T_n(t)$ are the Chebyshev polynomial functions given by

$$T_n(t) = \cos(n \arccos(t)). \tag{A4}$$

An outline of Chebyshev approximation methods and numerical routines for their application are given by Press *et al.* (1986). The N values for the C_k are solved for by matching the traction boundary condition at N Gauss–Legendre points along the crack faces. For the two problems solved in this study, a value of $N = 10$ gives satisfactory convergence of the results.

Quantities solved for

Once the solution is obtained for each problem by solving for the unknown $b(\xi)$, the fracture mechanics quantities

$$K_I = (2\pi)^s \frac{\mu_1}{2(1-\nu_1)} \lim_{\xi \to a_0} (b(\xi)\xi^s) \tag{A5}$$

and

$$\delta(y) = \int_{a_0}^{y} b(\xi)\, d\xi \tag{A6}$$

are extracted, where K_I is the mode I stress intensity factor and $\delta(y)$ is the crack opening displacement.